

The dynamics of spatio-temporal droughts in Northeast Brazil

Joao Dehon Pontes Filho^{1,2}, Francisco Assis de Souza Filho², Ályson Brayner Souza Estácio¹, Ticiania Marinho de Carvalho Studart², Eduardo Sávio Passos Rodrigues Martins¹

¹Research Institute for Meteorology and Water Resources (FUNCEME), 60115-221 Fortaleza-CE, Brazil

²Hydraulic and Environmental Engineering Department (DEHA), Federal University of Ceará (UFC), 60020-181 Fortaleza-CE, Brazil.

Correspondence to: Joao D. Pontes Filho¹ (joao.pontes@funceme.br)

Código de campo alterado

Abstract.

Droughts are complex spatiotemporal phenomena that challenge effective monitoring and response. This study introduces a novel analytical framework that simplifies drought characterization. Building on three-dimensional (3D) drought analysis, we introduce three new evolution metrics—Growth Curve, State Curve, and Dynamic Curve. This framework allows clear assessment of drought evolution through its expansion, persistence, and contraction phases. Applied to Northeast Brazil, a semi-arid region with recurrent severe droughts, the method identified four main typologies of drought progression. Most droughts in the region exhibit a characteristic pattern of rapid expansion, long persistence, and abrupt contraction, reflecting a typical signature of regional climate variability. Recognizing such recurrent evolution patterns provides decision-makers with an evidence-based understanding of how droughts tend to evolve, supporting more timely and region-specific management actions. The proposed framework thus bridges the gap between scientific drought analysis and practical preparedness planning, breaking the complexity dilemma of scientific information that is hard to apply in operational applications. Its flexible structure can be adapted to other drought indices and regions, offering a transferable tool to strengthen proactive drought governance worldwide.

Highlights

1. Proposes Growth Curve, State Curve, and Dynamic Curve to systematically track drought expansion, persistence, and contraction.
2. Identifies four distinct drought evolution typologies, improving predictability and proactive planning.
3. Reveals that Type II droughts (rapid expansion, long persistence, abrupt contraction) are the most prevalent in Northeast Brazil, giving insights in how to plan for proactive drought management.

Keywords:

Drought Analysis; Drought Evolution; Drought Typology

1 Introduction

Droughts can exhibit significant spatial heterogeneity, with their severity and affected area changing over time (Andreadis et al., 2005; Vicente-Serrano, 2006). Despite their spatio-temporal nature, early studies on drought characterization focused primarily on the temporal dimension, often using run theory to analyze drought events independently from the original time series (Yevjevich V, 1967; Espinosa et al., 2019; Liu et al., 2019). To incorporate spatial variability, researchers began using regionalization techniques such as Thiessen polygons and statistical clustering methods like Principal Component Analysis (PCA) and K-means (Portela et al., 2015; Zhou et al., 2019). However, these approaches represent spatial variability through fixed regional partitions (administrative or statistically derived), which can obscure the continuous and shifting spatial footprint of drought as it propagates. In contrast, more recent object-based space–time event approaches treat drought as evolving clusters in longitude–latitude–time, without requiring predefined boundaries.

Alongside these developments, drought events have long been characterized through attributes such as duration, deficit volume (severity), minimum intensity and related metrics, typically derived from event definitions based on thresholds or index time series (e.g., Fleig et al., 2006; Sutanto and Van Lanen, 2020; Yang et al., 2018). These descriptors underpin a broad body of drought frequency and risk-assessment studies, including multivariate formulations that explicitly account for dependence between key characteristics (e.g., duration and severity) rather than treating them in isolation (e.g., Pontes Filho et al., 2020; Shiau, 2006). While essential to quantify magnitude and recurrence, such summaries inevitably compress each event into a small set of aggregate descriptors and therefore provide limited diagnostic information on how an event unfolds internally (e.g., when it shifts from rapid expansion to persistence or contraction).

Complementary to these event summaries, spatio-temporal drought research has developed event-based tracking and clustering approaches that follow drought footprints in longitude–latitude–time, enabling the analysis of moving, merging and splitting clusters and the derivation of trajectory-related diagnostics. Here, we use “3D” as shorthand for this event-based tracking in longitude–latitude–time,

following the terminology adopted in previous clustering/tracking studies, while acknowledging that the broader concept is widely referred to as spatio-temporal drought analysis. Building on this established literature, our focus is not on introducing spatio-temporal tracking per se, but on addressing a remaining gap: providing an interpretable intra-event phase diagnostic (State, Growth and Dynamic curves), a typology of intra-event evolution, and probabilistic phase-transition information that can complement both aggregate descriptors and tracking-based descriptions.

Recent advancements in drought research have introduced methodologies capable of tracking drought movement in both space and time. Building on the concept of severity-area-duration (SAD) curves, proposed by Andreadis et al. (2005), subsequent studies have developed 3D clustering algorithms (longitude, latitude, and time) to analyze drought trajectories (Diaz et al., 2018, 2019; Herrera-Estrada et al., 2017; Herrera-Estrada and Diffenbaugh, 2020; Lloyd-hughes, 2012). However, a key limitation of many advanced 3D clustering methods, including those by Herrera-Estrada et al. (2017) and Diaz et al. (2019, 2020), is that while they provide robust tracking of drought dynamics and detailed statistical characterization of attributes like displacement, growth, and intensification rates, they often result in complex analytical outputs. These outputs, though scientifically rigorous, frequently emphasize descriptive statistics or intricate visual depictions that can be challenging for non-specialists to synthesize into structured, actionable insights for decision-making. For instance, Herrera-Estrada et al. (2017) meticulously analyze how drought clusters displace and change in area and intensity, but the focus remains on the statistical patterns of these dynamics rather than providing a simplified, diagnostic framework for event evolution.

Despite significant advances in drought analysis and monitoring, a fundamental challenge persists: adopting models that are either overly simplistic, failing to capture key spatiotemporal characteristics, or excessively complex, limiting their practical application for decision-makers. This "complexity dilemma" highlights the necessity for methodologies that strike a balance between analytical robustness and practical applicability in order to improve drought mitigation and adaptation strategies.

To overcome these limitations, researchers have increasingly adopted event-based frameworks that present spatio-temporal drought characteristics. For instance, Andreadis et al. (2005) introduced severity–area–duration (SAD) curves, which combine spatial extent and severity over different

90 durations to construct envelopes of extreme drought events. More recently, Chen et al. (2023) and Banfi et al. (2024) proposed the use of Normalized Area–Time Accumulation (NATA) curves, which allow retrospective evaluation of the temporal accumulation of drought-affected areas and provide insight into the phases of growth and recovery, an analytical step subsequent to event detection. This highlights the ongoing need for methodologies that can bridge the gap between complex scientific analysis and intuitive, decision-support tools, particularly in developing countries where resource limitations for complex data interpretation and advanced operational systems are often present. These methodologies represent significant advances in describing the magnitude and structure of historical spatio-temporal droughts, and they have also inspired typology-based classifications that cluster events with similar trajectories.

95 Recent cumulative-curve approaches, such as the NATA framework (Banfi et al., 2024; Chen et al., 2023), provide an elegant standardization to compare drought events of different durations by expressing their evolution in terms of normalized area and time and, in some applications, fitting the resulting curve with an analytical function to delimit broad stages (e.g., early growing, consolidation, exhaustion). This is useful for retrospective synthesis and inter-event comparison. However, because these
100 approaches primarily summarize each event through a single standardized cumulative trajectory, phase turning points are typically obtained indirectly (e.g., from properties of a fitted curve) and are not naturally expressed as a coupled set of state, integral, and derivative descriptors. Moreover, NATA-based typologies remain largely descriptive and do not explicitly quantify the likelihood of switching among drought phases. These limitations motivate our three-curve framework, which explicitly separates the
105 instantaneous drought state, its cumulative evolution, and its rate of change, enabling transparent identification of turning points and a probabilistic characterization of phase transitions.

In response to this persistent "complexity dilemma," this study proposes a novel framework that rebalances analytical robustness with practical applicability in 3D drought assessment. The explicit aim is to provide more structured and interpretable information to enhance drought evolution
110 characterization, giving insights into to proactive preparedness planning. In this study, we propose a three-curve analytical framework that advances the characterization of spatio-temporal drought dynamics by introducing three complementary measures: the State Curve (evolution of a drought characteristic such as affected area or severity), the Growth Curve (its cumulative integral), and the Dynamic Curve (its first

derivative). This framework enables droughts to be easily decomposed into expansion, persistence, and contraction phases, which are then used to define four distinct proposed typologies of drought evolution. Importantly, we further incorporate a transition matrix that quantifies the likelihood of moving between phases, providing a probabilistic representation of drought dynamics.

This structured framework then enables the proposition of actionable typologies of drought evolution, which serve as a simplified yet comprehensive classification system for decision-makers.

These typologies translate complex spatio-temporal dynamics into predictable behavioral patterns, offering more direct guidance for proactive planning by identifying how individual droughts are likely to evolve and persist. For instance, knowing that a region is predominantly affected by droughts with rapid expansion, long persistence, abrupt contraction behaviours can inform the design of early warning systems and resource allocation strategies, emphasizing quick response to onset and sustained support during the persistence phase. This level of practical applicability is a significant added value compared to existing 3D clustering methods that primarily focus on describing trajectories or broad event categories based on aggregated properties.

By simplifying complex spatio-temporal drought analyses into an accessible typology, this study contributes to bridging the gap between advanced analytical methods and the practical needs of decision-making in drought-prone regions. It complements and extends existing methodologies by introducing probabilistic information on changing drought evolution, thereby offering new tools for comparative research and for the long-term planning of drought risk management.

2 Materials and methods

The methodology to classify the evolution of drought events in the proposed typology follows these steps: 1) Definition of spatio-temporal droughts events; 2) Definition of spatio-temporal drought characteristics; 3) Analysis of drought event evolution using Three-curve model; 4) Classification of drought evolution according to proposed typologies; and 5) Probabilistic analysis of changing phase using transition matrix. Figure 1 shows the schematic workflow of the full procedure.

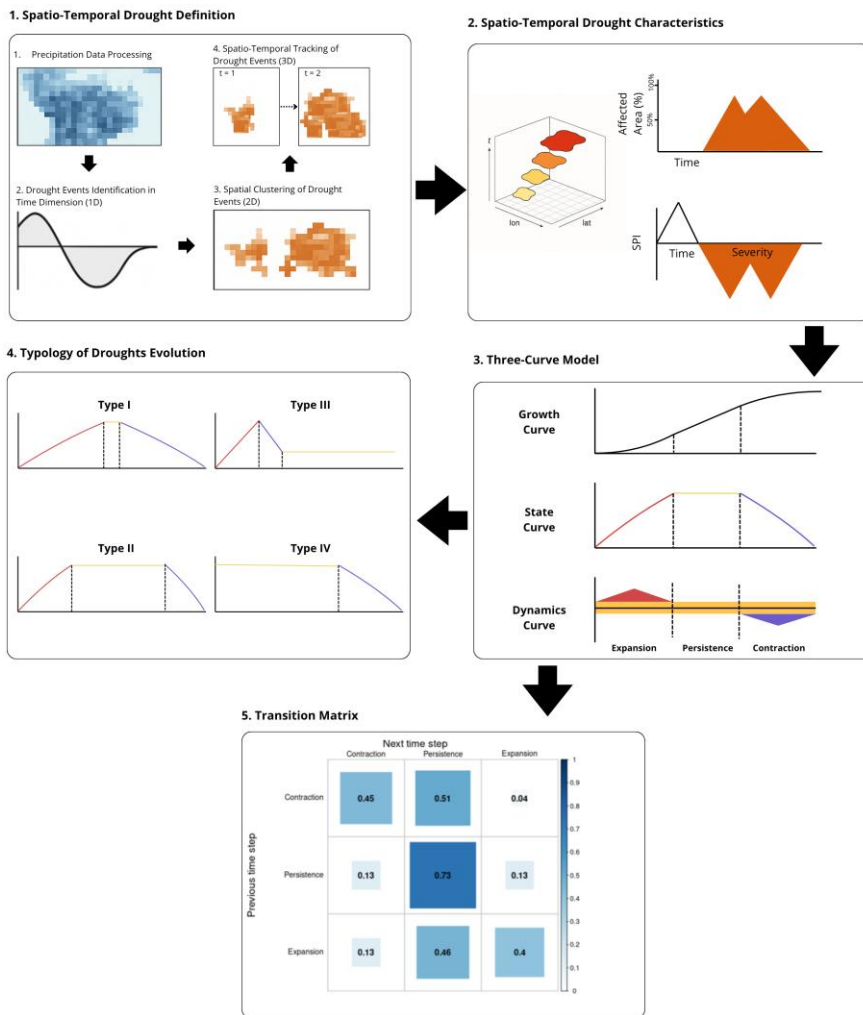


Figure 1: Schematic workflow proposed to classify the evolution of drought events. The first panel shows the definition of spatial-temporal drought events. The second shows the Three-curve model and the third panel show the proposed drought evolution typologies.

2.1 Spatio-Temporal Drought Definition

145 The spatio-temporal drought definition is divided into four steps: (i) Precipitation data processing; (2) Drought event identification in the time dimension (1D), (3) Spatial clustering of drought events (2D), and (4) Spatio-temporal tracking of drought events (3D).

Step 1: Precipitation Data Processing

150 The first step for drought spatio-temporal definition is data processing. It requires gridded data to support the spatial analysis. Monthly precipitation data were sourced from the CRU TS v4.05 dataset, which has a spatial resolution of $0.5^\circ \times 0.5^\circ$ and covers the period from 1950 to 2018 (Harris et al., 2020). Although the CRU TS v4.05 time series extends back to 1901, we opted to use data from 1950 onward due to the limited availability of rain gauge records in the study region during the early 20th century, which could introduce uncertainties in data interpolation.

155 The Standardized Precipitation Index (SPI) was calculated for each grid cell using a Gamma probability distribution fitted to the precipitation time series (Mckee et al., 1993). While SPI is widely recognized for its simplicity and comparability, its exclusive reliance on precipitation can be perceived as a limitation for fully capturing the complexities of multifaceted droughts, especially in light of modern advancements in drought assessment (Mishra and Singh, 2010). However, it is crucial to emphasize that
160 the primary objective of this study is to introduce and validate a novel methodological framework for spatiotemporal drought evolution analysis, rather than to advocate for a single, specific drought indicator.

For the Northeast Brazil (NEB) case study, SPI was deliberately chosen due to compelling regional data availability advantages. In NEB, precipitation data boast significantly longer historical series and a much denser monitoring network compared to other hydro-meteorological variables. For
165 instance, the meteorological network in NEB that measures evaporation represents approximately only 10% of the pluviometric network. This stark difference in data density and historical depth makes precipitation-based indices, particularly SPI, the most robust and reliable choice for demonstrating the capabilities of our spatiotemporal tracking methodology in this specific region. Therefore, while we acknowledge the increasing importance of multi-indicator approaches for comprehensive drought
170 characterization, especially for agricultural or hydrological impacts, the use of SPI in this context allowed

us to leverage the highest quality and most extensive historical data available for NEB to rigorously test our novel framework.

Also, since precipitation is the most widely available climatic variable, the World Meteorological Organization recommends using the Standardized Precipitation Index (SPI) for drought analysis (World Meteorological Organization, 2012). The SPI offers three key advantages: (i) it relies solely on precipitation, making it simple to calculate; (ii) it provides standardized values, allowing for easy regional comparisons; and (iii) it accommodates different timescales, making it applicable to agricultural, hydrological, and socioeconomic drought assessments (Hayes et al., 2007; Pontes Filho et al., 2019).

Despite the choice for using SPI, the proposed methodology is designed to be versatile and can be applied to any gridded time-series of a drought index. Future studies could incorporate additional indices such as SPEI (Standardized Precipitation Evapotranspiration Index) or PDSI (Palmer Drought Severity Index) to improve drought characterization as the methodology proposed in this study for the drought spatio-temporal analysis fits any gridded time-series of drought index and any drought definition.

Step 2: Identification of Drought Events in the Time Dimension (1D)

Run theory (Yevjevich, 1967) was applied to detect continuous periods in which SPI values remained ≤ -1.0 in each grid cell. ~~Drought perception varies among users, as water shortages impact different sectors at different times. Shorter time scales, such as 1 to 3 months, can be more critical to agricultural users who do not irrigate their cultures. Longer time scales, such as 6 to 12 months, may relate to hydrological impacts on urban and irrigation water supplies. Thus, the aggregation period and the threshold selected can strongly impact drought analysis. We used SPI-12 for our analysis as the region presents strong seasonality and it is highly dependent on pluriannual water reservoirs. Other aggregation periods can also be used; however, the resulting event trajectories and typology frequencies are expected to be time scale dependent (e.g., shorter scales such as SPI-1/SPI-3 typically exhibit less persistence and more intermittent evolution). Drought perception varies among users because precipitation deficits propagate through the hydrological system at different rates, affecting sectors at different times. Accordingly, the SPI was explicitly designed to quantify precipitation anomalies over multiple accumulation periods, which reflect drought impacts on different water resources: soil moisture typically~~

200 responds at relatively short timescales, whereas groundwater, streamflow, and reservoir storage integrate
longer-term precipitation anomalies (World Meteorological Organization, 2012). In practice, shorter
accumulation periods (e.g., 1–3 months) are often more relevant for rainfed agricultural systems, while
longer periods (e.g., 6–12 months) better capture hydrological implications for urban supply systems and
irrigated agriculture. Therefore, both the accumulation period and the threshold selected can strongly
205 influence drought identification and subsequent analyses. We adopted SPI-12 because the study region
exhibits strong seasonality and relies heavily on multi-annual reservoir storage; nevertheless, other
accumulation periods can be used, and the resulting event trajectories and typology frequencies are
expected to be time-scale dependent (e.g., shorter scales such as SPI-1/SPI-3 typically show lower
persistence and more intermittent evolution).

Step 3: Spatial Clustering of Drought Events (2D)

210 Each grid cell experiencing drought was analyzed spatially to identify clusters of connected drought areas. An 8-neighbor connectivity rule was applied, defining a drought cluster as a set of adjacent grid cells where $SPI \leq -1.0$ simultaneously in the same time-frame. To avoid identifying small, localized events, a minimum affected area threshold of 1.6% of the total study area was used (Xu et al., 2015).

215 More than one cluster of affected areas can occur at the same time-frame. At this step, they will only be considered as a single event if they are contiguous. However, this condition can change as we will see in step 4.

Step 4: Spatio-Temporal Tracking of Drought Events (3D)

The generation of these three-dimensional drought events, which inherently accounts for their spatial extent and temporal continuity, is achieved through a multi-step clustering and tracking algorithm.

220 Drought clusters were tracked over time to analyze their evolution and propagation paths. A drought event was considered continuous if at least 1.6% of its area overlapped between consecutive months. This specific overlap threshold was adopted in this study, consistent with established criteria used in previous spatiotemporal drought analyses by Li et al. (2020) and Xu et al. (2015). This choice reflects a common practice in the literature and this filter is important for distinguishing significant spatio-temporal
225 connections while filtering out minor, ephemeral overlaps that may not represent a continuous drought event. The overlap threshold controls whether consecutive monthly drought patches are linked into a

single event or split into multiple events. A larger (more stringent) overlap requirement generally yields shorter, more fragmented events, whereas a smaller (more permissive) threshold promotes longer, more merged events; by affecting event duration and cumulative metrics, this choice can alter the relative prominence of phases and thus potentially influence typology assignment.

In our framework, 3D drought events are constructed by first identifying 2D contiguous drought clusters at each time step (8-neighbour connectivity) and then linking clusters across consecutive months using an areal overlap criterion. This ‘tracking-by-overlap’ approach builds a 3D event as a time-ordered sequence of connected 2D slices, enabling explicit split/merge handling through the linkage rules. In contrast, other 3D clustering approaches define connectivity directly in the space–time domain (nearest neighbours forming a cube in space–time) and identify 3D connected components without an explicit overlap-based linkage stage (Diaz et al., 2020). We adopted the 2D+overlap tracking for transparency and control over temporal continuity while acknowledging that 3D connectivity-based clustering represents a valid alternative when a direct space–time connectivity definition is preferred.

Through this methodology, each drought event evolving in space and time is assigned to a unique ID. If, at some point, two distinct clusters coalesce at a future point in time, all cells that were previously identified as belonging to separate clusters will now be considered part of a single cluster. This transformation occurs even if these cells were not in direct contact with one another in the past. Consequently, it is possible for a single event to encompass regions that are not contiguous, provided that these regions have been in contact with one another at some point during the event's duration. The present approach entails the reclassification of all the clusters as belonging to the same larger event, on the basis that the driving climatic variables are the same (Andreadis et al., 2005). This procedure permits drought events to exhibit variability in both duration and spatial extent, and are not confined to a predefined climate region.

An important consideration in the proposed algorithm is that when a cluster splits into two or more clusters, they all retain the same initial ID. This is a modification of the algorithm used by Diaz et al. (2019) and Herrera-Estrada et al. (2017), whose analysis only preserved the areas of the largest clusters. We chose this path because droughts can occur simultaneously in different regions due to different precipitation mechanisms affecting each region. Therefore, conserving only the largest area may

255 artificially interrupt an event that is still occurring or even completely ignore an event that occurred
simultaneously but in different regions.

2.2. Spatio-Temporal Drought Characteristics

260 ~~Drought characteristics represent the various dimensions through which drought events
manifest and evolve across time and space, including their duration, severity and affected area (Fleig et
al., 2006; Sutanto and Van Lanen, 2020). Each characteristic provides a complementary perspective:
severity indicates the magnitude of the water deficit; the affected area reflects the spatial extent of the
phenomenon; duration captures its persistence. Understanding these characteristics individually enables
researchers and practitioners to identify not only when and where a drought occurs, but also how it
265 develops and what impacts it may generate across different sectors. Such a multidimensional perspective
enhances the responsiveness of decision makers, allowing them to anticipate critical phases, prioritize
vulnerable regions, and design targeted mitigation and adaptation strategies that improve drought
preparedness and resilience.~~

~~To analyze how a single drought characteristic evolves during events' duration, an intra event
270 analysis is performed. In this study, we choose to analyze two drought characteristics: affected area and
severity.~~

~~In this study, only affected area and severity were selected as the primary characteristics for
assessing drought dynamics, as the objective is to perform an intra event analysis that focuses on the
evolution of drought behavior throughout its duration. The affected indicates the overall reach of the
drought event in a given moment. Severity is defined as the average of SPI values across the grid cells
275 clustered as one drought event in each moment. Unlike duration, which represents the temporal extent of
an event and is inherently captured by the tracking of its onset and termination, affected area and severity
provide complementary and dynamic insights into how droughts expand, persist, and contract over time.
The affected area reflects the spatial dimension of drought propagation, while severity quantifies the
280 intensity of the deficit within the affected region.~~

Affected area: At each time step t (i.e., each month in the analysis period), the affected area of a tracked drought event k is computed as the percentage of the study domain covered by the set of grid cells assigned to that event. Let $\Omega_k(t)$ denote the set of grid cells that compose event k at month t , a_i the area of grid cell i , and N the total number of grid cells in the study domain. The affected area AA (in %) is then defined as:

$$AA_k(t) = 100 \times \frac{\sum_{i \in \Omega_k(t)} a_i}{\sum_{i=1}^N a_i},$$

where $\sum_{i \in \Omega_k(t)} a_i$ is the total area covered by event k at month t , and $\sum_{i=1}^N a_i$ is the total study-domain area.

For a regular grid with equal-area cells, this expression simplifies to:

$$AA_k(t) = 100 \times \frac{n_k(t)}{N},$$

where $n_k(t)$ is the number of cells composing event k at month t and N is the total number of grid cells in the study domain.

Severity: Event severity at month t is defined as the mean SPI-12 value over the cells composing the event footprint at that month. Let $SPI_{i_k}(t)$ denote the SPI-12 value at grid cell i and month t , and let $n_k(t)$ be the number of cells in event k at month t . Severity S is computed as:

$$S_k(t) = \frac{1}{n_k(t)} \sum_{i \in \Omega_k(t)} SP I_i(t),$$

2.3. The Three-Curve Model

Each drought characteristic, in this study the affected area and severity, was used to compute the three-curve model. For each tracked drought event k , we apply the three-curve model to each drought characteristic previously defined—namely, affected area $AA_k(t)$ and severity $S_k(t)$ —to describe how that characteristic evolves over the course of the event.

Formatado

Formatado: Inglés (Estados Unidos)

Formatado: Inglés (Estados Unidos)

Formatado

Formatado: Inglés (Estados Unidos)

Formatado: Inglés (Estados Unidos)

Formatado: Inglés (Estados Unidos)

Formatado: Inglés (Estados Unidos)

Formatado: Inglés (Estados Unidos)

Formatado

Formatado: Inglés (Estados Unidos)

Formatado

Formatado: Inglés (Estados Unidos)

Formatado: Inglés (Estados Unidos)

Formatado: Inglés (Estados Unidos)

Formatado: Inglés (Estados Unidos)

Formatado

Formatado: Inglés (Estados Unidos)

Formatado

Formatado: Inglés (Estados Unidos)

Formatado: Inglés (Estados Unidos)

Formatado: Inglés (Estados Unidos)

Formatado: Inglés (Estados Unidos)

Formatado

Formatado: Inglés (Estados Unidos)

Formatado

Formatado: Inglés (Estados Unidos)

Formatado: Inglés (Estados Unidos)

Formatado

Formatado: Fuente: (Padrão) Liberation Serif

Formatado: Inglés (Estados Unidos)

Formatado: Inglés (Estados Unidos)

Formatado

Formatado

1. **State curve:** the time series of the drought characteristic itself, $X_k(t)$.
2. **Growth curve:** the cumulative sum of the state curve over time (i.e., the discrete-time accumulation of $X_k(t)$ along the event duration).
3. **Dynamic curve:** the first temporal derivative of the state curve, computed in discrete time as the month-to-month change in $X_k(t)$.

Formatado: Inglês (Estados Unidos)

Formatado: Inglês (Estados Unidos)

Formatado: Inglês (Estados Unidos)

Formatado: Inglês (Estados Unidos)

Formatado: Inglês (Estados Unidos)

Formatado: Inglês (Estados Unidos)

~~1. Growth Curve: Cumulative of drought characteristics (Integral of State Curve).~~

~~2. State Curve: Drought characteristics.~~

~~3. Dynamic Curve: Change in state curve (1st derivative of State Curve).~~

The three-curve model represents an adaptation of an analytical framework originally proposed by Utsunomiya et al (2020) for monitoring the spread of COVID-19. In their study, the authors introduced three metrics: growth curve, growth rate, and acceleration, which in the present study correspond to the growth curve, state curve, and dynamic curve, respectively. We adopt this terminology because, unlike epidemic monitoring, where the cumulative count (growth curve) is typically the primary variable of interest, our analysis focuses on the evolution of the drought characteristic itself (state curve). Referring to $X_k(t)$ as a “rate” would therefore be misleading, and consequently its first derivative should not be interpreted as “acceleration”. This terminological modification was necessary because, in the context of COVID-19, the primary monitored variable was the growth curve. Conversely, in this study, the monitored variable is the state curve, making it inappropriate to refer to it as a rate and, consequently, to define its first derivative as acceleration.

To further characterize the spatiotemporal evolution of each event, we introduce a Drought Phase Classifier based on the dynamic curve. Specifically, the classifier assigns one of three phases to each time step: expansion (D^+), persistence (D^0), or contraction (D^-). This classification provides a direct interpretation of whether the drought characteristic value is increasing, remaining approximately stable, or decreasing through time. Because affected area and severity capture different dimensions of drought behavior, the phases are computed independently for each characteristic; thus, within the same event, area may be expanding while severity is contracting (or vice versa). ~~To better characterize the spatiotemporal evolution of drought events, we introduce the Drought Phase Classifier, a methodology~~

Formatado: Fonte: Não Negrito, Inglês (Estados Unidos)

Formatado: Fonte: Não Negrito, Inglês (Estados Unidos)

Formatado: Fonte: Não Negrito, Inglês (Estados Unidos)

Formatado: Fonte: Não Negrito, Inglês (Estados Unidos)

335 based on the Dynamic Curve, which represents the first derivative of the State Curve. This classifier provides insights into the dynamic phase of a drought event by categorizing it into one of three possible phases: contraction (D^-), persistence (D^0), or expansion (D^+). Understanding these phases enables a more precise evaluation of drought behavior and facilitates understanding whether a drought characteristic is intensifying, maintaining its characteristic or dissipating. Each characteristic, such as affected area or severity, exhibits independent behaviour, meaning that within a single drought event, one
340 characteristic may be expanding while another is contracting.

In order to define the transition between phases, the dynamic curve values of each event were normalized, and thresholds of 0.75 and -0.75 were used. The rationale for the selection of this procedure was to emphasise the moments at which the drought characteristic evolves most rapidly within the event, to ascertain whether the characteristic is expanding, persisting or contracting. Consequently, the rate of
345 evolution between these events was not deemed to be a priority at this juncture.

2.4. Typology of Droughts Evolution

To better understand the different ways in which droughts evolve over time, a typology of
350 drought events was developed based on their State Curves evolution patterns. Four theoretical models of drought evolution were proposed here, each representing a distinct way in which the affected area and severity evolve throughout the event. These typologies provide insight into how droughts expand, persist, and contract, helping to better understand drought evolution in a specific region and proactively plan accordingly. The four typologies (Types I–IV) are introduced in this study as conceptual archetypes for classifying intra-event evolution trajectories derived from the three-curve framework. They are not
355 intended as a consolidation of a single pre-existing typology from the literature, but as an interpretable set of templates describing how drought events can evolve through expansion, persistence, and contraction.

Typology assignment was performed through visual template-matching (Figure, 1, Panels 3–4). For each drought event, we compared the observed State Curve $X_i(t)$ shape (for affected area and severity) against the four theoretical evolution templates (Types I–IV) shown in Fig. 1 (Panel 4), based

Formatado: Texto

Formatado: Fonte: Não Negrito

Formatado: Fonte: Não Negrito

Formatado: Fonte: Não Negrito

Formatado: Fonte: Não Negrito

365 ~~on the relative prominence and sequencing of expansion, persistence, and contraction phases derived from the three-curve model (Figure 1, Panel 3). Typology assignment was performed through visual template-matching. For each drought event, we compared the observed State Curve shape (for affected area and severity) against the four theoretical evolution templates (Types I-IV), based on the relative prominence and sequencing of expansion, persistence, and contraction phases.~~ Two authors independently assigned each event (or event segment) to the best-matching typology; disagreements were resolved through joint review and consensus. When a single event exhibited clearly distinct evolution patterns over its lifetime, the event was segmented into successive sub-periods and each segment was classified separately. Figure 1 shows the four proposed typology graphical behaviors, that are better explained below:

Formatado: Fonte: Não Negrito

Formatado: Fonte: Não Negrito

Formatado: Fonte: Não Negrito

370

Type I: Prolonged Expansion, Rapid Persistence, and Prolonged Contraction

The Type I model represents a simplified conceptualization of droughts as slow-onset, creeping phenomenon. In this case, droughts expand gradually, experience a short persistence phase, and then enter a long contraction phase before completely dissipating. This model aligns with the idea that 375 droughts are progressive and cumulative phenomena, following a pattern that often influences societal responses according to the hydro-illogical cycle (Wilhite, 2012). As the event unfolds, it triggers gradual awareness, progressing from alert to concern and ultimately panic as impacts intensify. However, real-world droughts often deviate from this idealized behavior, necessitating additional typologies to describe more complex evolution patterns.

380

Type II: Rapid Expansion, Prolonged Persistence, and Rapid Contraction

The Type II model describes droughts that expand quickly, leading to a long period of persistence, followed by a rapid contraction phase. This behavior contrasts with the gradual expansion seen in Type I and reflects situations where drought conditions develop abruptly, often due to sudden precipitation deficits or extreme climatic anomalies. The extended persistence phase suggests that the 385 drought remains severe for an extended period, making it particularly impactful on water resources, agriculture, and ecosystems. The rapid contraction phase indicates that when recovery begins, it happens relatively quickly, likely due to intense rainfall events or large-scale climatic shifts.

Type III: Rapid Expansion and Contraction with Prolonged Persistence

In the Type III model, droughts undergo a short-lived expansion phase, followed by a
390 similarly short contraction phase. However, rather than dissipating entirely, the drought enters a prolonged
persistence phase, maintaining its intensity over an extended period. This type of drought suggests a lag
in the expected precipitation, resulting in a rapid expansion, but when the rainfall finally comes, it results
in a also rapid contraction, partially alleviating but not sufficiently to terminate the event. The long
persistence phase that follows implies that the affected region remains under drought stress. This pattern
395 is particularly relevant in regions where intermittent rainfall events are insufficient to break prolonged
dry conditions, leading to extended periods of water scarcity and socioeconomic stress.

Type IV: Instantaneous Maximum Expansion and Rapid Contraction

The Type IV model represents droughts that begin with their maximum State Curve, followed
by a long persistence phase, and end with a rapid contraction. This type can be considered a special case
400 of Type II, but without a distinct expansion phase. The fact that these droughts immediately start at full
intensity suggests that they may be triggered by sudden climatic shifts, such as the abrupt onset of long-
term precipitation deficits. Their extended persistence phase means that they pose significant long-term
challenges for water resource management, while their rapid contraction indicates that recovery, when it
comes, is swift and driven by a major meteorological shift.

405 2.5 Transition Matrix for Drought Phase

To evaluate the continuity of drought phases over time and their likelihood of transitioning
between phases, we employed a Transition Matrix approach. This method provides a probabilistic
framework to quantify the evolution of drought dynamics by analyzing the frequency with which an event
remains in the same phase or shifts to another phase in the subsequent time step.

410 The Transition Matrix T represents the probability of a drought event moving from one phase
at time step t to another phase at time $t + 1$.

The transition probabilities are calculated based on the historical dataset, where the relative
frequency of transitions between phases is used to estimate the likelihood of each possible phase change
(Cancelliere et al., 2007; Estácio et al., 2021). The transition matrix is defined as:

$$T = \begin{matrix} P(D^+ \rightarrow D^+) & P(D^+ \rightarrow D^0) & P(D^+ \rightarrow D^-) \\ P(D^0 \rightarrow D^+) & P(D^0 \rightarrow D^0) & P(D^0 \rightarrow D^-) \\ P(D^- \rightarrow D^+) & P(D^- \rightarrow D^0) & P(D^- \rightarrow D^-) \end{matrix}$$

where $P(A \rightarrow B)$ represents the probability of transitioning from phase A at time t to phase B at time $t + 1$.

The transition probabilities were computed empirically by analysing all drought events in the historical record and counting the occurrences of each transition type. The probabilities were determined using the following equation:

$$P(A \rightarrow B) = \frac{N(A \rightarrow B)}{N(A)}$$

where:

$N(A \rightarrow B)$ is the number of times a drought event transitioned from phase A to phase B .

$N(A)$ is the total number of occurrences of phase A in the dataset.

2.6 Study Area and Data

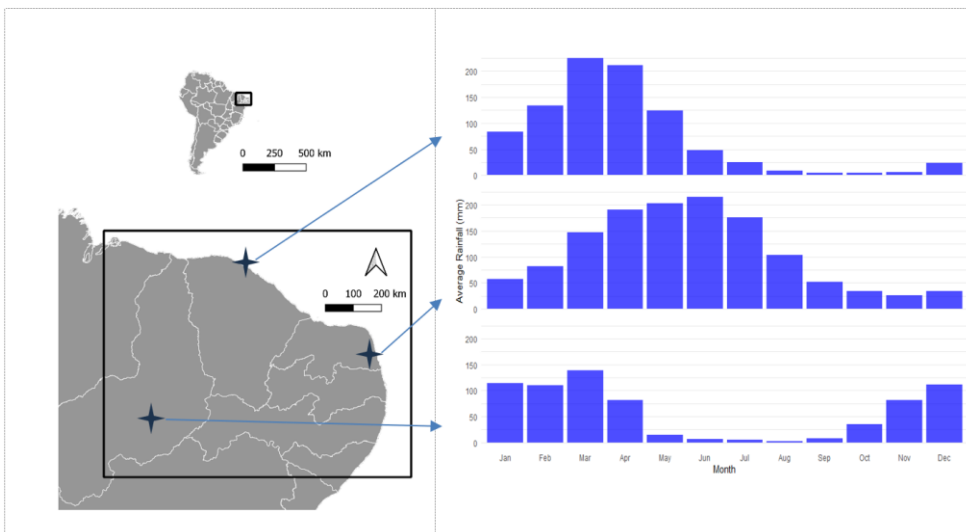
The northern portion of Northeast Brazil (NEB), was chosen as a case study to demonstrate the proposed framework as it is a semi-arid region that frequently experiences recurrent droughts due to its high climatic variability. This region, located between 2° and 10°S and 34° and 44°W, is primarily influenced by the Intertropical Convergence Zone (ITCZ), which is the main driver of precipitation in majority of the study area (Hastenrath, 2012; Moura and Shukla, 1981; Uvo et al., 1998).

Despite the ITCZ influence, other distinct climatic mechanisms also influence different subregions of NEB. Figure 2 illustrates the seasonality of precipitation in NEB, highlighting the distinct ~~seasonalities~~ seasonality associated with different climate drivers. In the northern part, there is a pronounced rainy season from February to May, associated with the southward migration of the ITCZ. Additionally, a pre-seasonal rainfall period occurs in December and January, while dry conditions dominate the remaining months. The eastern coastline, although also impacted by the ITCZ, receives its primary rainfall input from the Southeast Trade Winds between May and July. Meanwhile, the southernmost areas, particularly in the southwest, experience rainfall due to Cold Fronts from November

440 to January, with additional contributions from the ITCZ between February and April (Hastenrath and Heller, 1977; Uvo et al., 1998). These atmospheric systems modulate drought occurrence and evolution across the region, making it essential to understand their roles in shaping precipitation patterns.

The impact of the ITCZ on drought conditions in the region is a complex phenomenon, influenced by a variety of interrelated factors. This descent is influenced by two main phenomena: the El Niño Southern Oscillation (ENSO) in the Pacific Ocean and the Interhemispheric Tropical Atlantic Gradient (IHTAG) in the Atlantic Ocean (Andreoli and Kayano, 2005; Hounsou-Gbo et al., 2019; Nobre and Shukla, 1996). The ENSO and IHTAG have been identified as factors that can perturb Walker and Hadley cells, thereby inducing drifts in the ITCZ and, consequently, modifying the intensity and periodicity of the rainy season within the region.

450



455 **Figure 2: Location map showing the northern portion of Northeast Brazil (NEB). The rainfall charts are representative of the northern zone influenced by ITCZ, the eastern zone influenced by Southeast Trade Winds, and the southern zone influenced by Cold Fronts. Rainfall data CRU TS v4.05 from 1950 to 2018.**

3 Results

3.1 Drought Spatio-Temporal Definition

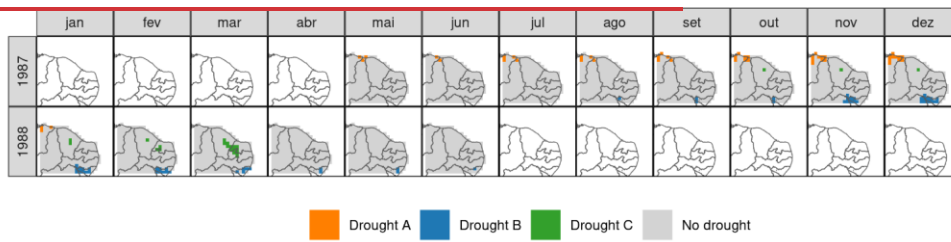
460 Understanding how droughts evolve within an event is critical for improving real-time monitoring and early warning systems. While spatio-temporal drought analyses have been developed for decades, many operational monitoring products and many synthesis communications still present drought conditions as time-slice maps and/or fixed-boundary regionalization; our framework complements these approaches by providing interpretable intra-event evolution diagnostics, typologies, and probabilistic
465 phase transitions. By identifying key moments of expansion, contraction, or persistence of severity and affected area in drought progression, this approach provides actionable insights for water resource management.

The 3D spatio-temporal drought definition algorithm enables the delineation of the cluster of contiguous cells that are affected by the same drought event, even in the case of simultaneous drought
470 events, i.e., those that occur in the same time interval but never coalesce.

This capability is illustrated in Figure 3, which depicts three separate drought events within the study area: Event A, which lasted from May 1987 to January 1988 and was located in the northwestern portion of the study area; Event B, which occurred between August 1987 and June 1988, affecting the southwestern region; and Event C, which lasted from October 1987 to March 1988 and was concentrated
475 in the central-northern sector of the study area.

Importantly, Figure 3 should not be interpreted as a generic gridded SPI-12 map. It represents the output of an object-based event definition and tracking procedure, in which contiguous drought cells are grouped into spatial clusters at each time step and then linked across consecutive months to construct drought events as evolving objects in longitude–latitude–time. This event-based representation is required
480 to consistently separate coexisting drought objects that occur in the same month, to track their individual evolution (movement, growth/shrinkage), and to account for possible future coalescence between initially isolated clusters, which would otherwise be lost in a purely time-slice depiction and would affect cumulative affected-area measures and event trajectories. In this context, a key difference in our

implementation relative to previous object-based frameworks (e.g., Diaz et al., 2019; Herrera-Estrada and
485 Diffenbaugh, 2020) is that we retain and track all drought objects detected at each time step, allowing
multiple events to evolve simultaneously in distinct regions. This is relevant because secondary objects
may later merge with larger ones and because simultaneous droughts can reflect distinct climatic drivers
operating across sub-regions of the domain.



490

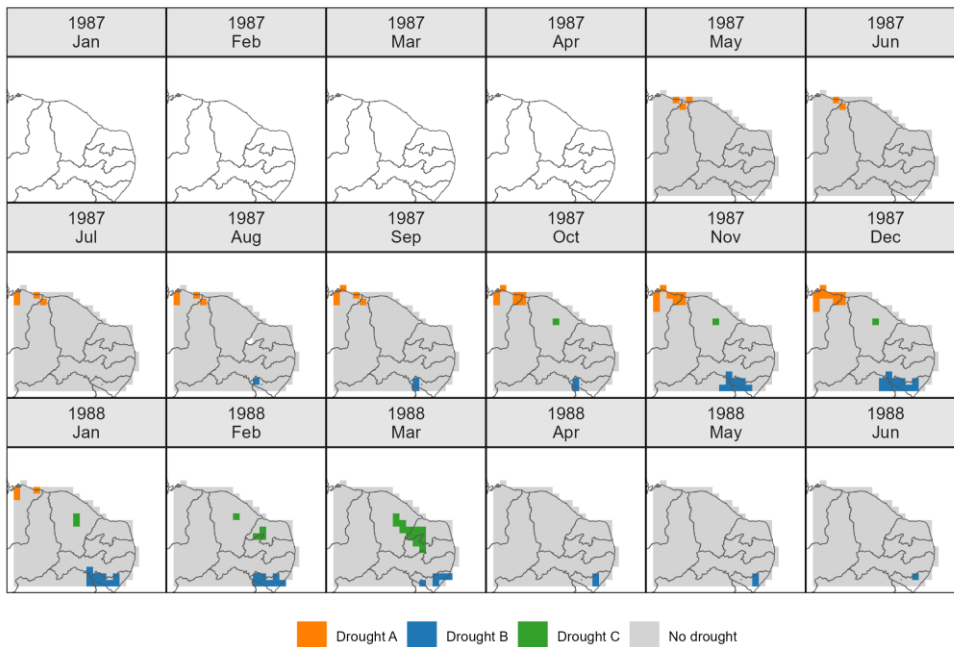


Figure 3: Example of simultaneously occurring drought events identified by the space-time clustering and tracking algorithm. Colored patches denote drought clusters belonging to different event IDs at each time step. White indicates no grid cells meet the drought criterion at that time step (non-drought) for the entire study domain, and grey denotes the non-drought grid cells when exists at least one drought event at that time step.

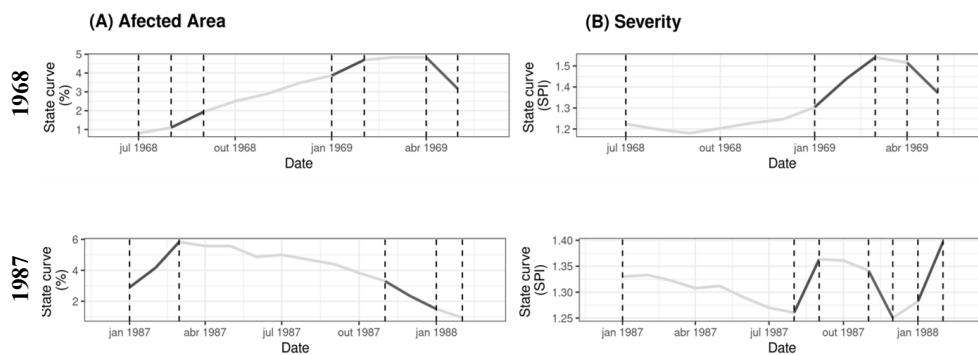
By distinguishing and evaluating individual drought events that impacted different regions at the same time, the algorithm provides a more specific understanding of drought dynamics, acknowledging that different parts of the study area are influenced by distinct precipitation-generating mechanisms. This is particularly relevant in Northeast Brazil, where the Intertropical Convergence Zone (ITCZ), Southeast Trade Winds, and cold fronts drive precipitation patterns in different sub-regions (Costa et al., 2018; Hastenrath, 2012; Nobre and Shukla, 1996; Uvo et al., 1998).

The ability to isolate co-occurring drought events is especially valuable for large-scale analysis, such as continental and global drought assessments, where simultaneous droughts in different regions could be driven by varied climatic drivers and teleconnections. This methodological enhancement allows for more precise drought characterization, ultimately contributing to improved monitoring, forecasting, and mitigation strategies.

3.2. Drought Spatio-Temporal Characteristics

The 3D cluster-based analysis of drought events allows for a comprehensive evaluation of their spatial and intensity characteristics. In this study, we assess two independent variables: (i) affected area, defined as the percentage of the total study area that is contiguously under drought conditions at a given time, and (ii) severity, measured as the mean SPI value of all grid cells within the drought cluster at that moment. These two characteristics provide complementary perspectives on drought evolution, as they do not necessarily follow the same trajectory over time.

The independent behavior of affected area and severity has important implications for drought monitoring and decision-making. While, in some cases, these variables exhibit strong agreement, with severity increasing as the affected area expands, in other cases, they follow divergent patterns, indicating that spatial extent and drought intensity may evolve differently throughout an event. Figure 4 highlights this contrast by presenting the evolution of these two characteristics in two distinct drought events. In the first case, the 1968-1969 event, both affected area and severity increased simultaneously, suggesting that the drought not only expanded but also intensified over time. In the second case, the 1987-1988 event, however, affected area and severity evolved in opposite directions, with one increasing while the other remained stable or even decreased.



525 **Figure 4: The evolution of the two drought characteristics analyzed, affected area, and severity, for the 1987 drought event over time.**

This discrepancy underscores the importance of considering both variables simultaneously in drought assessments. A drought that affects a large area but maintains moderate severity may affect the alternative water sources that could be shared to mitigate impacts, whereas a highly severe drought within a more localized area may pose acute agricultural productivity. Thus, relying solely on one of these indicators could lead to an incomplete understanding of drought impacts, reinforcing the need for a multidimensional approach in monitoring, forecasting, and management strategies.

3.3. Application of the Three-Curve Model

To enhance the understanding of drought evolution ~~at the event scale and facilitate decision-making~~, a drought phase classifier was developed, ~~introduced at Section 2.3~~. This classifier enables the identification of different phases of a drought event, categorizing moments in which a drought characteristics—affected area or severity—are expanding, persisting, or contracting, ~~based on the dynamic curve (i.e., the first derivative of the state curve) from the three-curve model~~.

In the three-curve representation (Figure 6), the state curve depicts the temporal evolution of the characteristic itself (affected area in %, or severity as the event-average SPI-12), the growth curve shows its cumulative behaviour over the event lifetime, and the dynamic curve highlights month-to-month

Formatado: Fonte: Não Negrito

Formatado: Fonte: Não Negrito

Formatado: Fonte: Não Negrito

Formatado: Fonte: Não Negrito

Formatado: Fonte: Não Negrito

changes and the resulting phase classification. In Figure 6, coloured segments indicate the identified phases (expansion, persistence, contraction), while vertical dashed lines mark phase transitions.

Figures 5 and 6 jointly illustrate the 1990–1994 drought event. Figure 5 provides the spatio-temporal drought map, where drought-affected cells are highlighted at each month, allowing the reader to track the spatial footprint of the event through time. Figure 6 presents the corresponding three-curve representation for affected area (panel A) and severity (panel B), linking the spatial evolution observed in Figure 5 to the temporal trajectories and phases detected by the classifier.

As shown in the maps (Figure 5), the event started with a small and fragmented footprint and then expanded rapidly in December 1990, covering a large portion of the study region. December typically coincides with the onset of the pre-rainy season; however, in 1990 this rainfall did not occur, affecting a large proportion of the study domain, which is consistent with the sharp expansion phase detected in the dynamic curves for the affected area (Figure 6, Panel A). By March 1991, with the onset of the rainy season, the drought footprint began to fragment and contract (Figure 5), yet these separated patches were still tracked as the same event because they reconnected later in time. From 1992 to January 1993, the event remained largely concentrated in the northwestern portion of the domain (Figure 5), corresponding to a predominantly persistent phase in both state curves (Figure 6). At the beginning of 1993, another rainy season failed to deliver sufficient precipitation, triggering a new expansion in both affected area and severity (Figure 6), which is also evident as a rapid growth of the drought footprint in the maps (Figure 5). Subsequently, the event remained broadly persistent until 1994, when the return of seasonal rainfall led to a rapid contraction of both characteristics (Figure 6) and the disappearance of drought conditions by May 1994 (Figures 5 and 6).

The classification is based on the dynamics curve, the last component of the three curve model, which represents the first derivative of the state curve. The state curve itself is defined as the state variable of the drought characteristics itself. Additionally, the growth curve offers an integrated view of the accumulated impact of the drought, making it easier to visualize the evolution of the affected area (percentage wise) and the cumulative severity over time.

By defining these phases and structuring the three curve model — growth curve, state curve, and dynamics curve — decision makers can easily interpret how historical drought events evolved. This

Formatado: Fonte: Não Negrito

Formatado: Fonte: Não Negrito

Formatado: Fonte: Não Negrito

Formatado: Fonte: Não Negrito

Formatado: Fonte: Não Negrito

Formatado: Fonte: Não Negrito

Formatado: Fonte: Não Negrito

Formatado: Fonte: Não Negrito

Formatado: Fonte: Não Negrito

Formatado: Fonte: Não Negrito

Formatado: Fonte: Não Negrito

Formatado: Fonte: Não Negrito

Formatado: Fonte: Não Negrito

Formatado: Fonte: Não Negrito

570 structured approach not only provides insights into drought evolution but also supports proactive
decision making, allowing authorities to plan mitigation measures specifically tailored to how droughts
evolve in their regions.

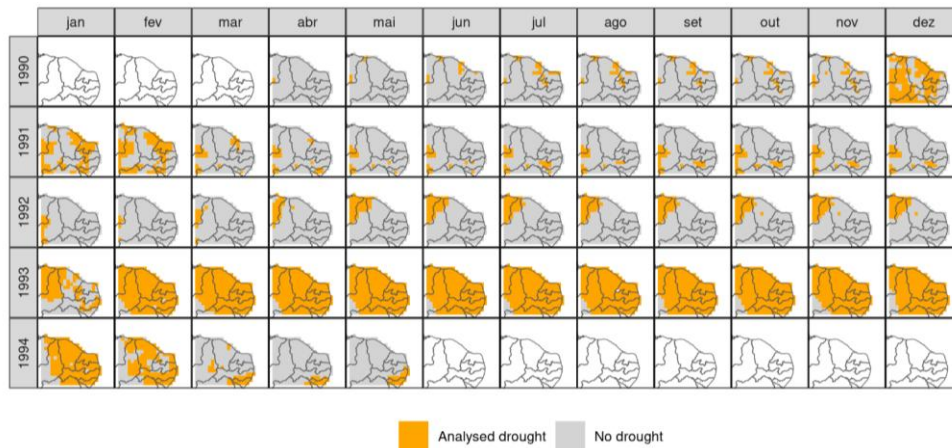
Figure 5 and 6 illustrate an example of the visualization of a drought event using the three-
curve model. The growth curve reflects the cumulative drought severity and affected area, the state curve
575 provides the current drought status, and the dynamics curve captures transitions between expansion,
persistence, and contraction phases. It also presents the spatio-temporal evolution map to facilitate
understanding of how the affected area evolved during the event.

By comparing the spatio-temporal evolution of the drought in the map and with the 3 curves
model, it is easy to understand that the event initially started small but expanded rapidly in December
580 1990, covering a large portion of the study region. The month of December is characterized by the onset
of the pre-rainy season, a period that typically is expected some amount of precipitation that precedes the
main precipitation period. However, this year was an exception, as precipitation was absent during this
time, thereby marking the commencement of the expansion phase. By March 1991, with the onset of the
rainy season, the drought began to fragment, becoming restricted to fewer areas. The map shows small
585 fragments of droughts. These are still regarded as the same event, given the fact that they will be connected
in the future. In 1992, the event remained concentrated in the northwestern portion of the region, where
it persisted until January 1993. The analysis indicates that both the State Curves of the affected area and
the Severity demonstrate a persistent phase during this period. In the beginning of 1993, a new rainy
season failed to deliver sufficient precipitation, leading to another expansion of the drought, both in terms
590 of affected area and severity. Following this rapid expansion of the two characteristics, the state curves
remained in a persistent phase for a considerable period, until in 1994 there was a rapid contraction of the
two variables with the advent of the new rainy season, thereby bringing the drought event to a conclusion
in May of that year.

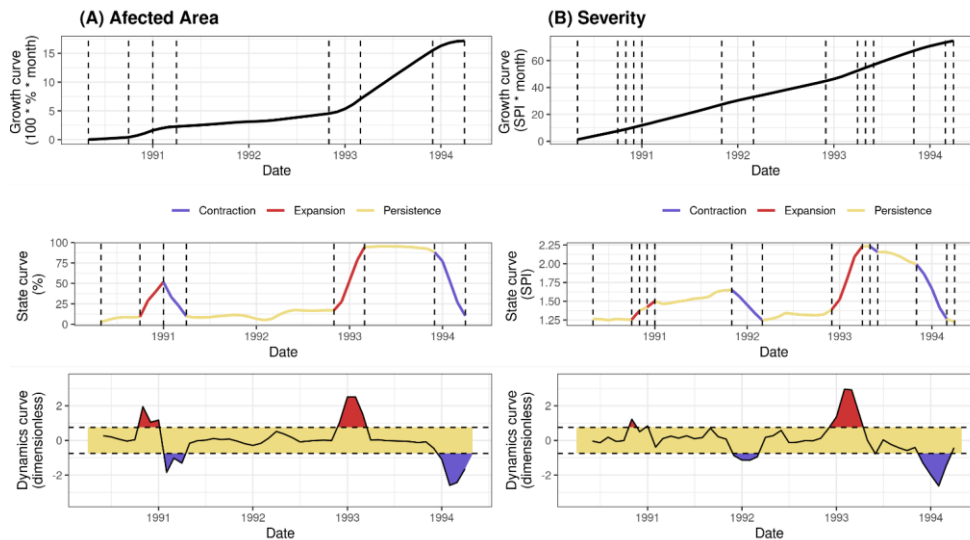
In this case, the affected area and severity exhibited similar behaviours (Figure 6), suggesting
595 a coupled relationship between spatial expansion and drought intensity. As the drought expanded spatially,
its severity also increased, while during the contraction phase, both variables simultaneously decreased.
This alignment indicates that the absence of the primary rain-producing mechanism during expected wet

Formatado: Inglés (Reino Unido)

600 periods not only increased the total affected area but also amplified drought severity. However, this is not a generalized behaviour across all drought events, as [better demonstrated throughout this study in section 3.5 using the transition matrix analysis](#). Therefore, monitoring these two variables is essential for an accurate understanding of drought progression and its potential impacts.



605 **Figure 5: Spatio-Temporal Drought Map of the 1990-1994 drought event over time. White indicates no grid cells meet the drought criterion at that time step (non-drought), and grey denotes the non-drought grid cells when exists at least one drought event at that time step.**



610 **Figure 6:** Spatio-Temporal Drought Map and 3 Curves Model for Affected Area and Severity, showing the evolution of the 1990–1994 drought event over time. Blue indicates the period when the variable is in Contraction, yellow denotes the Persistence, and red shows the expansion phase. Three-curve model and drought-phase classification for the 1990–1994 event, shown for (A) affected area and (B) severity. Colours indicate contraction (blue), persistence (yellow), and expansion (red); vertical dashed lines mark phase transitions.

3.4. Typology of Droughts Based on Evolution Dynamics

615 Using the 3D space-time drought analysis, we identified the 22 drought events. Since many of these events spanned multiple years, different dynamical evolution patterns could be observed within a single event. As a result, a total of 25 drought evolution classifications were visually assigned across the 22 events analyzed.

620 Figure 7 presents the four proposed theoretical types along with an observed case of affected area evolution for each typology. Type I, characterized by a long expansion phase, rapid persistence, and prolonged contraction, was observed in an event between October 1987 and April 1988. Type II, which exhibits rapid expansion, long persistence, and short contraction, is exemplified by an event spanning from 1987 to 1988. In this case, persistence occurred with a gradual decline, though not sufficiently steep to transition into the contraction phase for an extended period. It was only at the end of 1987 that the

625 transition to contraction occurred. Type III, defined by a rapid expansion followed by a swift contraction
and subsequent prolonged persistence, was observed in the year 1966. Finally, the 1961 event exhibited
a behavior similar to Type IV, which is characterized by an almost negligible expansion phase and long
persistence before contraction. In the observed case, the event showed intermittent alternations between
630 persistence and rapid expansion; however, overall, it followed the expected pattern of Type IV. It is
important to highlight that the theoretical models are not strictly adhered to in the observed cases, and a
visual assessment of each event is necessary to properly classify them within the proposed typology.

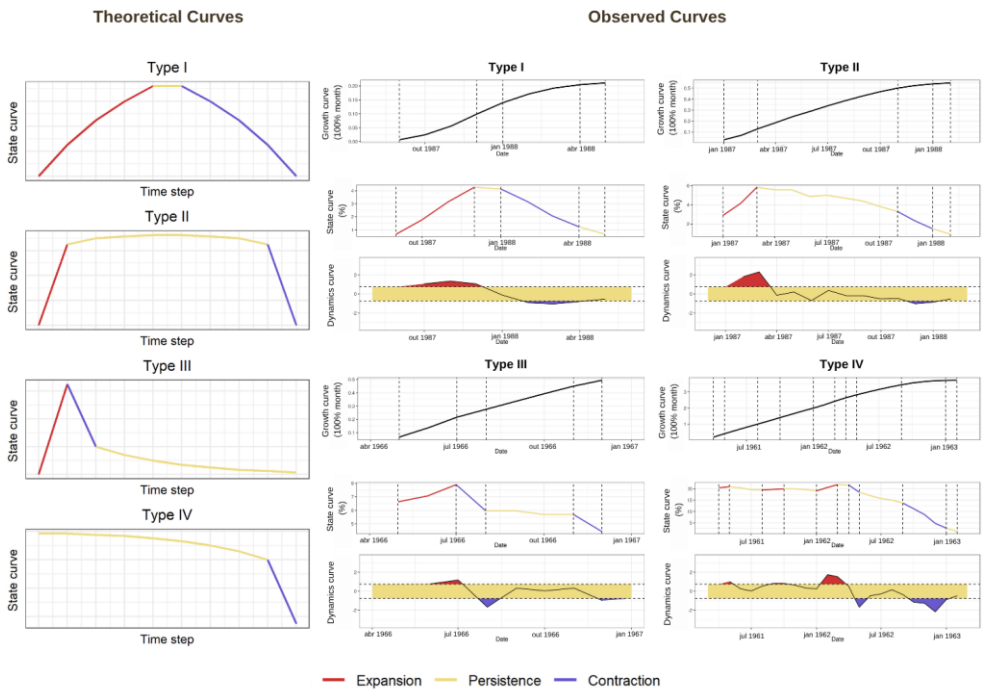
For the studied area, the most frequently observed drought type was Type II, representing 48%
of the cases. This was followed by Type III (24%), Type I (20%), and Type IV (8%). In terms of severity,
the dominance of Type II was even more pronounced, comprising 68% of classifications, while Type III,
635 Type IV, and Type I accounted for 20%, 8%, and 4%, respectively.

These results indicate that, for the study region and under the methodological framework used for drought
detection, Type II droughts—~~u~~ characterized by rapid expansion, long persistence, and rapid ~~contraction~~
~~recontraction~~, are the most prevalent form of drought evolution in the analyzed characteristics.

By knowing the predominant type of drought evolution in a specific region, decision-makers
640 can proactively plan accordingly to the expected behavior. ~~In the studied region, the predominance was
for Type II droughts.~~ This pattern can be attributed to the strong seasonality of precipitation in the region.
Approximately 80% of annual rainfall occurs within just four months, meaning that long dry periods are
a recurring feature of the climate. Additionally, the use of SPI-12 as the drought indicator, which
aggregates precipitation over a 12-month period, likely enhanced the persistence of events by smoothing
645 out short-term fluctuations and reinforcing the identification of extended drought periods.

The classification of drought evolution types provides valuable insights for policymakers,
water managers, and agricultural planners, as different drought dynamics demand different response
strategies.

Formatado: Recuo: Primeira linha: 0"



650

Figure 7: Theoretical and Observed Curves according to proposed typologies

The predominance of Type II droughts suggests a need for long-term preparedness and adaptive management strategies. Since these droughts expand rapidly, decision-makers must act early during the initial stages to implement mitigation measures before widespread impacts occur. The long persistence phase means that water resource planning and agricultural adaptation need to be structured for prolonged dry conditions. The rapid contraction at the end of these droughts highlights the importance of monitoring systems that can quickly detect recovery periods to optimize water release policies and agricultural replanting strategies.

655

Type IV, as a special case of Type II, also requires strong emphasis on rapid response mechanisms. Since these droughts immediately start at full, or almost full intensity, emergency measures

660

such as water rationing, agricultural subsidies, and drought relief programs may need to be deployed swiftly. Given their relatively short contraction phase, decision-makers should also ensure that recovery plans are synchronized with the return of wetter conditions, avoiding prolonged socio-economic disruptions.

665 Type I droughts, which involve gradual expansion, emphasize the need for sustained monitoring and proactive intervention, because adaptation measures should not be delayed to be implemented, at the risk of being too late to mitigate impacts. Type III occurs due to a late rainy season, and can strongly impact on the agricultural sector, with a lack of rainfall in the expected period. These droughts may initially appear less severe, but their persistence means that gradual depletion of water
670 resources and long-term agricultural stress can become major concerns.

By integrating this typology into drought preparedness plans, governments and institutions can enhance their ability to anticipate, monitor, and respond to droughts in a way that is tailored to the specific evolution pattern of each event. This approach reduces uncertainty, improves resource allocation, and strengthens the region's overall resilience to drought conditions.

675 Unlike operational monitoring tools such as Brazil's Drought Monitor, the proposed framework is explicitly an a posteriori method: it classifies droughts only after their full occurrence. Nevertheless, this retrospective perspective is valuable in two complementary ways. For researchers, it provides a structured and comparable language to analyze and classify droughts across regions and periods, complementing existing approaches such as SAD and NATA curves by emphasizing phase
680 dynamics rather than aggregated envelopes. For decision-makers, it offers an interpretable typology that highlights recurrent patterns of drought behavior. While not designed for real-time early warning, the identification of dominant drought types in Northeast Brazil provides insights that can inform drought preparedness planning, guide the design of water allocation policies, and support the tailoring of mitigation strategies to regional drought behaviors.

685 **3.5. Transition Matrix Analysis of Drought Phases**

To further investigate the temporal dynamics of drought evolution, a transition matrix was developed by pooling all drought events analysed in this study; results are presented in Figure 8. Rows

indicate the drought phase at time step t (previous time step), and columns indicate the phase at time step $t + 1$ (next time step). Therefore, each cell represents a conditional probability $P(\text{phase}_{t+1} = j \mid \text{phase}_t = i)$, and each row sums to 1. Values along the main diagonal represent the probability of remaining in the same phase from t to $t + 1$, whereas off-diagonal values represent the probability of transitioning to a different phase. The matrix should be interpreted row-wise (conditional on the current phase), rather than as a ranking from the lowest to the highest value across the entire matrix. Higher values along the diagonal indicate stronger phase persistence, whereas higher off-diagonal values indicate more frequent phase switching.

Example (severity): if an event is in persistence at month t , the matrix indicates a 0.73 probability of remaining in persistence at $t + 1$, and 0.13 probabilities of transitioning to expansion or contraction. Higher persistence probabilities are expected because, at a monthly time step, drought characteristics often exhibit temporal inertia, making persistence between consecutive months relatively frequent.

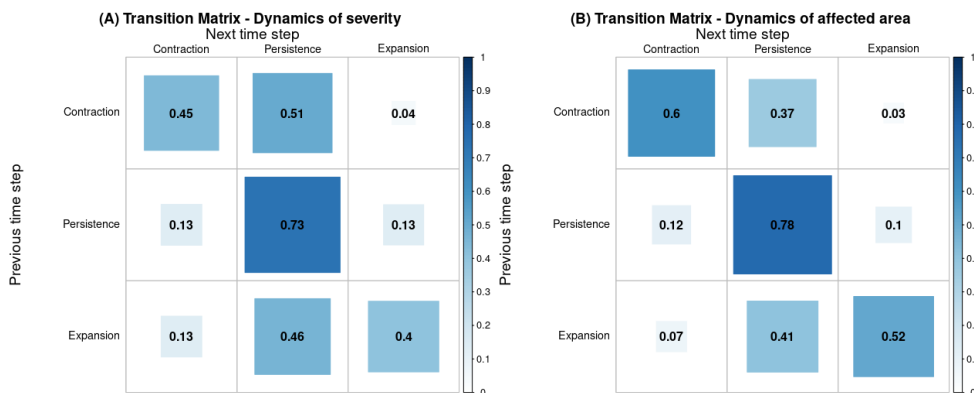


Figure 8: Transition matrix indicating the probability of a drought event remaining in the same phase or transitioning to another. Higher values along the diagonal suggest a strong persistence of each phase, whereas higher off-diagonal values indicate frequent transitions between phases.

When analysing Figure 8, the two variables exhibit distinct transition tendencies. For severity, the dominant pattern is that when the event is in expansion or contraction, the most likely transition in the next time step is toward persistence, rather than a direct switch to the opposite phase. This can be seen, for instance, in the contraction row (Figure 8, panel A): once the event is in contraction at time t , the probability of remaining in contraction at $t + 1$ is lower than the probability of transitioning to persistence ($P = 0.45$ vs 0.51). A similar tendency is found in the expansion row, where the probability of remaining in expansion is lower than the probability of transitioning to persistence ($P = 0.40$ vs 0.46). Overall, severity therefore shows more frequent phase switching, with rapid expansion or contraction often returning to a persistence stage.

In contrast, affected area displays higher phase retention. If the drought is in contraction at time t , it is more likely to remain in contraction at $t + 1$ ($P = 0.60$) than to shift to persistence or expansion ($P = 0.37$ and 0.03 , respectively) (Figure 8, panel B). The same tendency of higher diagonal probabilities (phase persistence) is also observed for the persistence and expansion rows. This quantitatively explains why affected area exhibits a more stable and consistent evolution: larger diagonal entries imply that the footprint is more likely to remain in the same phase from one month to the next. From a physical perspective, this reflects the spatial inertia of drought footprints: once drought conditions become spatially connected, the boundary of the affected area tends to expand or contract gradually in a spatially coherent manner, whereas severity (intensity within the footprint) can respond more rapidly to short-term rainfall variability, producing more frequent phase switches at monthly resolution.

Despite these differences, both variables share one dominant feature: when the drought event is in persistence at time t , it tends to remain in persistence at $t + 1$, with probabilities of 0.73 (severity) and 0.78 (affected area). This prominent persistence component is consistent with the typological assessment, in which Type II droughts, predominant in the region, are largely associated with persistent stages.

From an operational perspective, the higher short-term variability in severity suggests that severity-only signals may be more sensitive to transient fluctuations and may require careful interpretation when used as a primary indicator. In contrast, affected area appears more stable at a monthly

time step and may therefore provide a more robust indicator for monitoring the spatial evolution of drought impacts, with severity serving as a complementary measure of intensity.

These findings highlight the value of analysing drought characteristics separately: severity and affected area encode different dynamics. The tendency of severity to transition toward persistence suggests that intensity often stabilizes between periods of rapid strengthening or weakening, whereas the higher phase retention of affected area indicates more consistent spatial coverage patterns over time. Such insights are relevant for early-warning systems and adaptive drought management, as they help anticipate the most likely phase in the next time step conditional on the current phase.

4.1 Discussions

This study introduces a novel framework for analyzing spatiotemporal drought evolution, employing a three-curve model and a typology-based classification system derived from the dynamic behavior of drought characteristics. Our approach focuses on translating the complex outputs of 3D drought analysis into intuitive, actionable insights for drought monitoring and management. We found that Type II droughts, characterized by rapid expansion, prolonged persistence, and abrupt contraction, are the most prevalent in Northeast Brazil, a pattern attributed to the region's strong precipitation seasonality and the use of SPI-12.

The proposed framework is transferable to other aggregation periods and indices; however, the inferred event structure and the frequency of evolution typologies are expected to depend on the chosen time scale. In this study, SPI-12 emphasizes seasonal-to-interannual anomalies, which is consistent with a region strongly influenced by rainfall seasonality and multi-annual reservoir storage, and it tends to highlight persistence by smoothing short-term fluctuations. If shorter aggregation periods are adopted (e.g., SPI-1 or SPI-3), drought anomalies typically become more intermittent, with faster onset and recovery and greater fragmentation across consecutive time steps. Consequently, typologies dominated by long persistence are expected to become less prevalent, whereas rapid-evolution trajectories and more frequent phase switching (expansion–contraction cycling) are expected to occur more often. This time-scale dependence should be considered when interpreting typology results and when

760 transferring the framework to short-term monitoring, where shorter aggregation periods may be more appropriate.

The methodologies for analyzing spatiotemporal drought dynamics have evolved significantly. Classical approaches, such as Severity-Area-Duration (SAD) curves (Andreadis et al., 2005) offer aggregate statistics vital for climatological understanding and long-term planning. However, their aggregated nature often obscures intra-event dynamics critical for operational decision-making. For example, while a SAD curve provides the distribution of drought severity across different durations and areas for a population of droughts, it does not reveal the instantaneous phase (expansion, persistence, contraction) of a specific ongoing event. Our three-curve model explicitly addresses this gap by providing a diagnostic of how each drought event evolves, offering a process-oriented view not readily available from aggregate summaries.

775 More recent advancements, such as the 3D clustering algorithms developed by Herrera-Estrada et al. (2017) and Diaz et al. (2019), and the flexible DBSCAN-based approach by Cammalleri and Toreti (2023), provide sophisticated means to track drought trajectories and characterize their statistical properties (e.g., displacement distances, preferential pathways). Banfi et al. (2024), for instance, apply a generalized 3D clustering approach and NATA curves to classify European droughts into broad seasonal categories. While these methods generate rigorous scientific descriptions, they often present complex analytical outputs that require significant expertise to interpret into actionable insights.

Our framework is complementary to NATA-based analyses (Chen et al., 2023; Banfi et al., 2024) but differs in what it makes explicit for interpretation and decision support. In NATA, the event is summarized by a standardized accumulation curve and phases can be delineated from analytical properties of a fitted function, which provides a compact representation of temporal evolution. Here, instead, we treat drought evolution as a coupled signal system: the *State Curve* describes the instantaneous condition of a chosen drought characteristic, the *Growth Curve* accumulates its trajectory over the event lifespan, and the *Dynamic Curve* (first derivative) reveals turning points and phase boundaries directly from changes in the rate of evolution. This decomposition is not tied to a single cumulative template and can be applied consistently to different drought characteristics (e.g., affected area and severity), allowing comparisons of how multiple variables evolve within the same event. Importantly, by pairing phase

790 identification with a transition matrix, we move beyond descriptive staging and provide a probabilistic view of drought dynamics (i.e., the likelihood of remaining in or switching between expansion, persistence, and contraction), which is particularly relevant for proactive planning and early warning.

Our innovation lies in translating these complex dynamics into a simplified three-curve representation and a directly applicable typology of drought evolution. This allows for a more intuitive grasp of drought behavior, enabling stakeholders to anticipate future patterns without needing to interpret a multitude of complex metrics or delve into statistical clustering results themselves. Furthermore, our approach's commitment to preserving all concurrent drought clusters, even upon splitting, offers a more comprehensive representation compared to some prior methods (e.g., Diaz et al., 2019; Herrera-Estrada et al., 2017) that might prioritize only the largest cluster, potentially overlooking critical localized events, especially relevant for regions with diverse climatic drivers.

800 The explicit aim of this framework is to provide structured and interpretable information that provide insightful understanding of drought evolutions that can be used in proactive preparedness planning. Traditional drought-monitoring systems such as the North American Drought Monitor (NADM) (<https://droughtmonitor.unl.edu/>) and Brazil's Drought Monitor (<https://monitordesecas.ana.gov.br/>) serve primarily to track current drought conditions—mapping the spatial extent and intensity of drought in near-real-time (or at least on a monthly basis) in order to support operational decisions, based on hydro-meteorological indicators and verified with local institutions_ (Martins et al., 2016). By contrast, the methodology proposed here is not aimed at real-time operational monitoring, but rather at diagnosing how droughts evolve in time and space by focusing on intra-event dynamics (for example, expansion/shrinkage of the affected area and changes in severity within an event). In doing so, the tool can generate insights about typical behaviour patterns of drought events (e.g., how quickly severity increases, how the spatial footprint changes) that can inform proactive drought-management plans, rather than simply mapping current conditions for decision support. In other words, while existing monitors support situational awareness and trigger responses, our approach intends to support strategic planning by elucidating the regime of drought evolution—thereby enabling decision-makers to anticipate likely developments and craft management measures oriented to the typical progression of events rather than
815 only to detected states.

Código de campo alterado

While essential, these systems often lack a framework for systematically classifying and anticipating the evolutionary behavior of drought events. Our three-curve model and the derived typologies offer a diagnostic tool that can complement these systems by providing a deeper, process-oriented understanding of how a particular drought is likely to expand, persist, or contract. For example, 820 by identifying a newly emerging drought as a "Type II" event (rapid expansion, long persistence, abrupt contraction), decision-makers can be better informed to anticipate prolonged impacts and allocate resources for extended periods, rather than reacting solely to current conditions. This enables proactive measures, such as adjusting water usage policies, implementing crop diversification strategies, or preparing emergency aid, well in advance of peak impacts. The ability to categorize and understand these 825 distinct evolutionary pathways empowers managers to tailor response strategies more effectively, moving beyond purely reactive measures to more robust, anticipatory planning.

Despite its advancements, this study has limitations. First, the use of the CRU TS v4.05 dataset, with its 0.5° resolution, while providing a long historical record crucial for drought climatology, is acknowledged to be quite coarse for a region characterized by high spatial rainfall variability such as 830 Northeast Brazil. This resolution inherently limits the capture of fine-scale meteorological phenomena and highly localized drought events, potentially smoothing out micro-climatic patterns that could be relevant for very specific local impacts. While this choice was pragmatic given the need for a consistent, long-term dataset to demonstrate our methodological framework, future applications would greatly benefit from higher-resolution precipitation data (e.g., from regional models or downscaled products) to 835 enhance the precision of localized drought characterization. The reliance on SPI, though justified by data availability in NEB, means that the framework in this study primarily addresses meteorological drought, not directly incorporating the complexities of agricultural or hydrological droughts driven by temperature, evapotranspiration, or water storage changes. While the methodology is flexible enough to accommodate other indices, their direct application in this specific case study would require robust historical data, which 840 are currently less available. Furthermore, the assignment of drought events to typologies was performed visually, which, while guided by theoretical models, introduces a subjective element. Although effective for this initial methodological demonstration, an automated classification method for typology assignment would enhance objectivity and scalability for large datasets. Lastly, while the framework provides insights

into how droughts evolve, direct validation with decision-makers on its usability and impact on their management decisions is a necessary next step.

Because the present application is based on SPI-12, our event definition targets seasonal-to-interannual drought variability and is not designed to detect flash drought, which is commonly defined by rapid onset at shorter time scales (Sreeparvathy et al., 2025). However, the proposed framework is general and can be applied to shorter-scale indicators (e.g., SPI-1/SPI-3 or daily-scale SPEI/soil-moisture anomalies). Under such settings, flash droughts would be expected to produce trajectories with rapid expansion/onset, which would preferentially map to the rapid-expansion archetypes (Types II/III/IV), depending on whether a persistent phase develops or the event transitions rapidly into contraction. We therefore do not interpret the SPI-12 events analyzed here as flash droughts; the reference above is provided only to indicate how the framework could be transferred to shorter time scales.

This transferability shows how the framework proposed here can be easily adapted to other studies. Its core components—the 3D clustering algorithm, the three-curve model, the typology definition, and probabilistic information on phase switching—are independent of the specific drought index or geographical region. Any gridded time-series drought index can be used as input, allowing for application in diverse climatic zones and for various drought types (meteorological, agricultural, hydrological). This flexibility ensures that the methodology can be adapted to regions with different data availability and management priorities, making it a broadly applicable tool for enhancing drought monitoring worldwide.

Future work will focus on integrating additional climatic variables and testing alternative drought indices (e.g., SPEI, PDSI, soil moisture indicators) into the framework to provide a more comprehensive characterization of multi-faceted droughts. Efforts will also be directed towards developing automated classification algorithms for typology assignment to enhance objectivity and scalability. Crucially, direct engagement and validation with water managers and policymakers will be undertaken to refine the framework's practical utility and ensure its seamless integration into existing operational drought monitoring systems.

5. Conclusions

870 This study developed a spatio-temporal framework for drought classification, incorporating a 3D drought detection methodology, a three-curve model and the derived typologies of drought evolution to better understand how droughts evolve over time and space.

The application of the three-curve model—growth curve, state curve, and dynamics curve—proved to be a valuable tool for drought monitoring, allowing for a structured interpretation of drought expansion, persistence, and contraction phases. The transition matrix analysis further demonstrated that 875 drought affected area extent tends to remain stable within each phase, while severity exhibits greater variability, suggesting that affected area may be a more reliable indicator for decision-making.

By analyzing affected area and severity, we identified four distinct drought evolution typologies, and the study revealed that Type II droughts—characterized by rapid expansion, long 880 persistence, and abrupt contraction—are the most prevalent in the North of Northeast Brazil. The dominance of this drought type is likely influenced by the region’s strong precipitation seasonality, where rainfall is concentrated within a short period, and by the use of SPI-12, which enhances the persistence of events in the analysis.

From a management perspective, these findings highlight the importance of early detection, 885 long-term planning, and adaptive response strategies. Given the prevalence of rapid-expansion droughts, monitoring systems must be designed to detect early warning signs and enable proactive mitigation measures. Additionally, the prolonged persistence of droughts in the region reinforces the need for sustained water resource planning and agricultural adaptation policies.

This study provides a scientific foundation for improving drought monitoring and response 890 strategies, offering a methodology that can be applied to other semi-arid regions facing similar climatic challenges. Future research should focus on integrating additional climatic variables, testing alternative drought indices, and expanding the analysis to other geographic contexts. By refining these tools, policymakers and researchers can enhance early warning systems, strengthen resilience-building measures, and mitigate the long-term socioeconomic and environmental impacts of droughts.

895

Code and data availability

The code and data used in this study are available upon request by emailing the corresponding author.

Author contributions

900 Conceptualization, methodology and validation, J.D.P.F., ABSE, and F.d.A.S.F.; formal analysis, investigation, writing—original draft preparation, J.D.P.F., F.d.A.S.F., ABSE, and E.S.P.R.M.; software, J.D.P.F and ABSE.; writing—review and editing, supervision: F.d.A.S.F., E.S.P.R.M. and T.M.d.C.S.

Acknowledgements

905 We would like to thank the Federal University of Ceará (UFC) for their support in conducting this research, as well as the Ceará Foundation for Meteorology and Water Resources (FUNCEME) for their institutional support. We also acknowledge the financial support provided by CAPES (Coordination for the Improvement of Higher Education Personnel), which was instrumental in making this study possible.

910 Competing interests

The authors declare no conflict of interest.

Reference

- 915 Andreadis, K. M., Clark, E. A., Wood, A. W., Hamlet, A. F., and Lettenmaier, D. P.: Twentieth-century drought in the conterminous United States, *J. Hydrometeorol.*, 6, 985–1001, <https://doi.org/10.1175/JHM450.1>, 2005.
- Andreoli, R. V. and Kayano, M. T.: ENSO-related rainfall anomalies in South America and associated circulation features during warm and cold Pacific decadal oscillation regimes, *International Journal of Climatology*, 25, 2017–2030, <https://doi.org/10.1002/joc.1222>, 2005.
- 920 Banfi, F., Cammalleri, C., and Michele, C. De: A joint spatio-temporal characterization of the major meteorological droughts in Europe, *Environmental Research Letters*, 19, <https://doi.org/10.1088/1748-9326/ad6ba9>, 2024.
- Cammalleri, C. and Toreti, A.: A Generalized Density-Based Algorithm for the Spatiotemporal Tracking of Drought Events, *J. Hydrometeorol.*, 24, 537–548, <https://doi.org/10.1175/JHM-D-22-0115.1>, 2023.

- Cancelliere, A., Mauro, G. Di, Bonaccorso, B., and Rossi, G.: Drought forecasting using the standardized precipitation index, *Water Resources Management*, 21, 801–819, <https://doi.org/10.1007/s11269-006-9062-y>, 2007.
- 925 Chen, R., Liu, Y., Zhu, Y., Ren, L., Qu, Y., Otkin, J. A., and Singh, V. P.: A spatiotemporal deconstruction-based approach for identifying flash drought expansion: Normalized Area-Time Accumulation curve, *J. Hydrol. (Amst.)*, 621, <https://doi.org/10.1016/j.jhydrol.2023.129509>, 2023.
- Diaz, V., Corzo Perez, G. A., Van Lanen, H. A. J., and Solomatine, D.: Intelligent Drought Tracking for its Use in Machine Learning: Implementation and First Results, 3, 601–594, <https://doi.org/10.29007/klgg>, 2018.
- 930 Diaz, V., Corzo Perez, G. A., Van Lanen, H. A. J., Solomatine, D., and Varouchakis, E. A.: Characterisation of the dynamics of past droughts, *Science of the Total Environment*, 134588, <https://doi.org/10.1016/j.scitotenv.2019.134588>, 2019.
- Diaz, V., Perez, G. A. C., Lanen, H. A. J. Van, Solomatine, D., Varouchakis, E. A., and Varouchakis, E. A.: An approach to characterise spatio-temporal drought dynamics, Elsevier Ltd, 103512 pp., <https://doi.org/10.1016/j.advwatres.2020.103512>, 935 2020.
- Espinosa, L. A., Portela, M. M., Pontes Filho, J. D., Studart, T. M. de C., Santos, J. F., and Rodrigues, R.: Jointly modeling drought characteristics with smoothed regionalized SPI series for a small island, *Water (Switzerland)*, 11, 1–27, <https://doi.org/10.3390/w11122489>, 2019.
- Estácio, A. B. S., Oliveira, S. M., and Souza Filho, F. de A.: STATISTICAL UNCERTAINTY IN DROUGHT FORECASTING USING MARKOV CHAINS AND THE STANDARD PRECIPITATION INDEX (SPI), *Revista Brasileira de Climatologia*, 17, <https://doi.org/http://dx.doi.org/10.5380/abclima.v28i0.77590>, 2021.
- 940 Fleig, A. K., Tallaksen, L. M., Hisdal, H., and Demuth, S.: A global evaluation of streamflow drought characteristics, *Hydrol. Earth Syst. Sci.*, 10, 535–552, <https://doi.org/https://hess.copernicus.org/articles/10/535/2006/hess-10-535-2006.html>, 2006.
- Harris, I., Osborn, T. J., Jones, P., and Lister, D.: Version 4 of the CRU TS monthly high-resolution gridded multivariate climate dataset, *Sci. Data*, 7, 1–18, <https://doi.org/10.1038/s41597-020-0453-3>, 2020.
- 945 Hastenrath, S.: Exploring the climate problems of Brazil's Nordeste: A review, *Clim. Change*, 112, 243–251, [https://doi.org/38:2653–2675](https://doi.org/38:2653-2675), 2012.
- Hastenrath, S. and Heller, L.: Dynamics of climatic hazards in northeast Brazil, *Quarterly Journal of the Royal Meteorological Society*, 103, 77–92, <https://doi.org/10.1002/qj.49710343505>, 1977.
- 950 Hayes, M. J., Alvord, C., and Lowrey, J.: Drought Indices 2007, Intermountain West Climate Summary, 1–5, 2007.
- Herrera-Estrada, J. E. and Diffenbaugh, N. S.: Landfalling Droughts: Global Tracking of Moisture Deficits From the Oceans Onto Land, *Water Resour. Res.*, 56, <https://doi.org/10.1029/2019WR026877>, 2020.
- Herrera-Estrada, J. E., Satoh, Y., and Sheffield, J.: Spatiotemporal dynamics of global drought, *Geophys. Res. Lett.*, 44, 2254–2263, <https://doi.org/10.1002/2016GL071768>, 2017.
- 955 Hounsou-Gbo, G. A., Servain, J., Araujo, M., Caniaux, G., Bourlès, B., Fontenele, D., and Martins, E. S. P. R.: SST indexes in the tropical South Atlantic for forecasting rainy seasons in Northeast Brazil, *Atmosphere (Basel)*, 10, <https://doi.org/10.3390/atmos10060335>, 2019.

- Li, J., Wang, Z., Wu, X., Xu, C. Y., Guo, S., and Chen, X.: Toward monitoring short-term droughts using a novel daily scale, standardized antecedent precipitation evapotranspiration index, *J. Hydrometeorol.*, 21, 891–908, <https://doi.org/10.1175/JHM-D-19-0298.1>, 2020.
- 960 Liu, Y., Zhu, Y., Ren, L., Singh, V. P., Yong, B., Jiang, S., Yuan, F., and Yang, X.: Understanding the Spatiotemporal Links Between Meteorological and Hydrological Droughts From a Three-Dimensional Perspective, *Journal of Geophysical Research: Atmospheres*, 124, 3090–3109, <https://doi.org/10.1029/2018JD028947>, 2019.
- Lloyd-hughes, B.: A spatio-temporal structure-based approach to drought characterisation, 418, 406–418, <https://doi.org/10.1002/joc.2280>, 2012.
- 965 Martins, E. S., Silva, R. F. V., Biazeto, B., and Quintana, C. M.: Northeast Drought Monitor: The Process, in: *Drought in Brazil: Proactive Management and Policy*, edited by: Erwin De Nys, Nathan L. Engle, A. R. M., CRC Press, 2016.
- McKee, T. B., Doesken, N. J., and Kleist, J.: The relationship of drought frequency and duration to time scales, *AMS 8th Conference on Applied Climatology*, 179–184, <https://doi.org/citeulike-article-id:10490403>, 1993.
- 970 Mishra, A. K. and Singh, V. P.: A review of drought concepts, *J. Hydrol. (Amst.)*, 391, 202–216, <https://doi.org/10.1016/j.jhydrol.2010.07.012>, 2010.
- Moura, A. D. and Shukla, J.: On the Dynamics of Droughts in Northeast Brazil: Observations, Theory and Numerical Experiments with a General Circulation Model, *J. Atmos. Sci.*, 38, 2653–2675, [https://doi.org/10.1175/1520-0469\(1981\)038<2653:otdodi>2.0.co;2](https://doi.org/10.1175/1520-0469(1981)038<2653:otdodi>2.0.co;2), 1981.
- 975 Nobre, P. and Shukla, J.: Variations of Sea Surface Temperature, Wind Stress, and Rainfall Over the Tropical Atlantic and South America, *J. Clim.*, 9, 1996.
- Pontes Filho, J. D., Portela, M. M., Marinho de Carvalho Studart, T., and Souza Filho, F. de A.: A Continuous Drought Probability Monitoring System, CDPMS, Based on Copulas, *Water (Basel)*, 11, 1925, <https://doi.org/10.3390/w11091925>, 2019.
- 980 Pontes Filho, J. D., Souza Filho, F. de A., Martins, E. S. P. R., and Studart, T. M. de C.: Copula-Based Multivariate Frequency Analysis of the 2012–2018 Drought in Northeast Brazil, *Water (Basel)*, 12, 834, <https://doi.org/10.3390/w12030834>, 2020.
- Portela, M. M., dos Santos, J. F., Silva, A. T., Benitez, J. B., Frank, C., and Reichert, J. M.: Drought analysis in southern Paraguay, Brazil and northern Argentina: regionalization, occurrence rate and rainfall thresholds, *Hydrology Research*, 46, 792–810, <https://doi.org/10.2166/nh.2014.074>, 2015.
- 985 Shiau, J. T.: Fitting drought duration and severity with two-dimensional copulas, *Water Resources Management*, 20, 795–815, <https://doi.org/10.1007/s11269-005-9008-9>, 2006.
- Sreeparvathy, V., Debdut, S., and Mishra, A.: A Review of Advances in Flash Drought Research: Challenges and Future Directions, <https://doi.org/10.1029/2025EF006603>, 1 August 2025.
- Sutanto, S. J. and Van Lanen, H. A. J.: Hydrological Drought Characteristics Based on Groundwater and Runoff across Europe, in: *Proceedings of the International Association of Hydrological Sciences*, 281–290, <https://doi.org/10.5194/piahs-383-281-2020>, 2020.

Utsunomiya, Y. T., Utsunomiya, A. T. H., Torrecilha, R. B. P., Paulan, S. de C., Milanesi, M., and Garcia, J. F.: Growth Rate and Acceleration Analysis of the COVID-19 Pandemic Reveals the Effect of Public Health Measures in Real Time, *Front. Med. (Lausanne)*, 7, 1–9, <https://doi.org/10.3389/fmed.2020.00247>, 2020.

995 Uvo, C. B., Repelli, C. A., Zebiak, S. E., and Kushnir, Y.: The Relationships between Tropical Pacific and Atlantic SST and Northeast Brazil Monthly Precipitation, *J. Clim.*, 551–562, 1998.

Vicente-Serrano, S. M.: Spatial and temporal analysis of droughts in the Iberian Peninsula (1910-2000), *Hydrological Sciences Journal*, 51, 83–97, <https://doi.org/10.1623/hysj.51.1.83>, 2006.

World Meteorological Organization: Standardized Precipitation Index: User Guide, 2012.

1000 Xu, K., Yang, D., Yang, H., Li, Z., Qin, Y., and Shen, Y.: Spatio-temporal variation of drought in China during 1961–2012: A climatic perspective, *J. Hydrol. (Amst)*, 526, 253–264, <https://doi.org/10.1016/j.jhydrol.2014.09.047>, 2015.

Yang, J., Chang, J., Wang, Y., Li, Y., Hu, H., Chen, Y., Huang, Q., and Yao, J.: Comprehensive drought characteristics analysis based on a nonlinear multivariate drought index, *J. Hydrol. (Amst)*, 557, 651–667, <https://doi.org/10.1016/j.jhydrol.2017.12.055>, 2018.

1005 Yevjevich V, I. J.: An objective approach to definitions and investigations of continental hydrologic droughts, Colorado State University, Fort Collins, 1967.

Zhou, H., Liu, Y., and Liu, Y.: An Approach to Tracking Meteorological Drought Migration, *Water Resour. Res.*, 55, 3266–3284, <https://doi.org/10.1029/2018WR023311>, 2019.

1010